Arabian Journal for Science and Engineering (2019) 44:8081–8093
https://doi.org/10.1007/s13369-019-03995-4

RESEARCH ARTICLE - MECHANICAL ENGINEERING

Flow Analysis of Multilayer Gravity-Driven Sisko Fluid over a Flat Inclined Plane

Sumanta Chaudhuri[1] · Paromita Chakraborty[2] · Bitanjaya Das[2] · Ram Karan Singh[3]

Received: 4 November 2018 / Accepted: 24 June 2019 / Published online: 9 July 2019

Abstract
Gravity-driven thin film flow of two immiscible non-Newtonian Sisko fluids over a flat inclined plane is investigated. The equation, describing the flow, is nonlinear in nature and does not have a closed form of solution in general. In this study, the nonlinear governing differential equations are solved analytically by employing homotopy perturbation method (HPM). Besides, an exact solution for a special case of the non-Newtonian index is also obtained. The results of the solution based on HPM are compared with the exact solution for the special case, and it shows close agreement between the two results. This demonstrates the efficacy of HPM for solving nonlinear problems. The expression for the velocity is obtained, and the effects of various parameters like Sisko fluid parameters, density ratio, and viscosity ratio are also analyzed and discussed. The results indicate that with increase in the density ratio, it causes a significant increase in the velocity of fluids in both the layers and the velocities in both the layers are decreasing significantly with an increase in the Sisko fluid parameters. This study has got wider application in various industrial activities such as protective and decorative coating, painting.

Keywords Gravity-driven flow · Sisko fluid · Thin film flow · Homotopy perturbation method · Multilayer flow

1 Introduction

Gravity-driven thin film flow of fluids down an inclined plane has attracted researchers over the years due to its widespread applications in various industrial applications such as protective and decorative coating, painting, etc. This coating process includes coating of papers of various grades, protective coatings of magnetic storage media such as the audio and video tapes, optical storage media like audio- and photo-compact disk, etc. This coating process may be of monolayer or multilayers. The properties of the coating depend on the number of layers and properties of individual coating material used in each layer. Studies [1] on coatings reveal that the multilayer coatings have better wear resistance and resistance to fracture than monolayer coatings. To ensure quality products, the film thickness should be uniform throughout the entire coating region. This uniformity is possible if any sort of flow disturbance dies out rapidly. Therefore, for a better quality of these products, the study of flow stability is very important and essentially requires the knowledge of the basic state of this flow process. Knowing the basic state, the effect of various parameters on the velocity distribution can be investigated. Velocity distribution is significantly affected by the pertinent parameters such as the density ratio of the fluids, ratio of the viscosity of the fluids, thickness ratio, etc., which play a crucial role in the final success of the coating process. Several researchers have investigated thin film flow of Newtonian fluid over flat and wavy inclined planes [1–3].

In many natural and industrial processes, however, the fluid involved is non-Newtonian in nature. The general terminology for non-Newtonian fluid applies for a very large number of fluids which deviate from Newtonian behavior in a diverse way. It is obvious that all such behaviors cannot be described by a single model or a single mathematical description. Depending on the rheological behaviors, several physical models have been suggested over the years. Based on this, several classes of fluid such as power-law fluid, Oldroyd-6, Ellis fluid, third-grade and fourth-grade

✉ Sumanta Chaudhuri
sumanta.chaudhurifme@kiit.ac.in

[1] School of Mechanical Engineering, Kalinga Institute of Industrial Technology (Deemed to be Univeristy), Bhubaneswar 751024, India

[2] School of Civil Engineering, Kalinga Institute of Industrial Technology (Deemed to be Univeristy), Bhubaneswar 751024, India

[3] Department of Civil Engineering, King Khalid University, Abha 61421, Saudi Arabia

fluid, Johnson–Segalman fluid, Sisko fluid, etc., have been conceived [4–6].

Single-layer thin film flow of non-Newtonian fluids through different geometries has been studied by the researchers. Gravity-driven flow of a power-law fluid down an inclined plane has been investigated by Amouche et al. [4]. Thin film gravity-driven flow of an Ellis fluid has been studied [5] numerically by implicit finite difference scheme. Alam et al. [6] investigated non-Newtonian Johnson–Segalman fluid flow over a vertical moving belt and cylinder for lifting and drainage problem. The nonlinear governing differential equations have been solved by the Adomian decomposition method (ADM) [6, 7], and the effect of pertinent parameters on the velocity distribution has been discussed. Thin film gravity-driven flow of a third-grade fluid [8] down an inclined plane has been examined, and an analytical solution for the velocity field employing traditional perturbation method and homotopy perturbation method has been obtained. The effect of various parameters on the velocity distribution has been discussed. The same problem has been studied by the researchers [9], and exact solution for the nonlinear governing equation has been developed. Kumaran et al. [10] investigated thin film gravity-driven flow of a third-grade fluid down an inclined plane and yielded exact solution and analytical solution for the equation governing the flow phenomenon. A correction of the previous [9] results has been introduced in the study of Kumaran et al. [10].

The studies, cited above, clearly indicate the importance of studying thin film gravity-driven flow of non-Newtonian fluids over an inclined plane. Sisko fluid is a non-Newtonian fluid model, put forward by Sisko [11], which is a three-parameter model. Cement slurries, paintings of different grades, and coating materials are some of the fluids observed to follow the Sisko model. Numerous researchers have studied flow of Sisko fluids under various circumstances which are of practical interest. Khan et al. [12], in a very recent paper, investigated irreversibility associated with the flow and heat transfer in Sisko nanomaterial employing homotopy analysis method (HAM) [12]. The effect of various parameters on the rate of entropy generation is investigated. Thin film flow of Sisko fluid over surface topography [13] has been studied numerically, and the effect of the pertinent parameters on the free surface profile has been investigated. Boundary layer flow of a Sisko fluid over a radially stretching sheet has been investigated [14]. Mixed convection heat transfer of a Sisko fluid over a radially stretching sheet has been studied [15]. HAM has been adopted for solving the governing equations, and the effect of various parameters on the flow and temperature field is discussed. Pulsatile flow of a Sisko fluid in an endoscope has been investigated by Nadeem et al. [16] both numerically and analytically. Flow of blood through a stenosed artery has been examined numerically by the researchers [17] modeling blood as a Sisko fluid. The effect of the rheological parameters on the velocity and flow rate is discussed. Siddiqui et al. [18] reported thin film flow of Sisko fluid and Oldroyd-6 fluid on a moving belt for lifting problem. Governing differential equations have been solved by HPM up to the second order, and the effect of the Sisko fluid parameter and the non-Newtonian index is discussed as well.

Though numerous researchers have investigated single-layer thin film flow of non-Newtonian fluid through various geometries, only a limited number of research work have been reported for multilayer flow of immiscible non-Newtonian fluids. However, such flow situations are also of importance in diverse engineering systems. Hajmohammdi et al. [19] carried out an analytical investigation of the two-layer Couette flow of a gas and power-law liquid in microcylinder and analyzed the effect of various parameters on the velocity field and temperature field. The present work is carried out to study the thin film flow of two immiscible non-Newtonian Sisko fluids over a flat, inclined plane. The novelty of the work lies in considering multilayer thin film gravity-driven flow of non-Newtonian Sisko fluids over an inclined plane, which has never been reported in the open literature. Exact solution of the governing equation in terms of the index n cannot be obtained due to the high nonlinearity of the equation governing the flow problem. In the present work, solution for the flow problem with two layers is obtained analytically by HPM [20, 21]. Though numerical techniques are capable of generating accurate results even for highly nonlinear problems, analytical solutions are always preferred to get a deeper understanding of the parametric dependencies of the dynamics of the phenomenon, presenting a better insight into the physics of the problem without compromising with the accuracy of the results. In the present study, HPM has been adopted to solve the nonlinear governing equations describing the flow phenomenon, and analytical solution for the non-dimensional velocity is obtained. The effects of the Sisko fluid parameter, density ratio, thickness ratio, and non-Newtonian index on the velocity have been discussed.

2 Problem Formulation

The geometry of the problem is shown in Fig. 1. Two immiscible non-Newtonian Sisko fluids, with different properties, flow down an inclined plane. The plane is inclined at an angle θ with the horizontal. The $\hat{x}$-axis is along the direction of the flow, and the $\hat{y}$-axis is perpendicular to the plane surface. The plane is considered very large in the $\hat{z}$-direction, which indicates that the width of the plane is large compared to the length of the plane. As a result, the end effect can be neglected and the effect of the velocity in the z-direction is negligible. This assumption indicates that the results of the present study are valid when the plane is very large in the z-direction. The

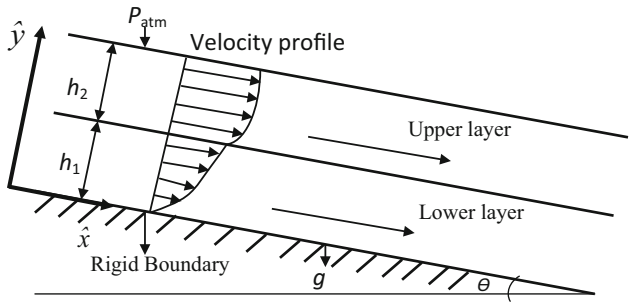

Fig. 1 Geometry of the flow of two immiscible Sisko fluids down a flat inclined plane

thickness of the film is very small in coating process. The flow is analyzed for the fully developed regime, which indicates that the plane is long enough in the axial direction to ensure fully developed condition. As a result, the velocity is independent of the coordinate in the axial direction and the length of the plane is not required in the analysis. The thicknesses of the bottom layer and top layer are h_1, h_2, respectively, and these are uniform. The flow is assumed to be steady, laminar, incompressible, and fully developed. The pressure acting on the top layer is atmospheric.

2.1 Governing Differential Equations

The equations governing the flow are obtained from the conservation of mass and momentum principle. The thermal effect is neglected as the flow is gravity-driven, and thus, the temperature is assumed to be constant. The mass and momentum conservation equations are as follows:

$$\nabla \cdot \vec{V} = 0 \tag{1}$$

$$\rho\left[\frac{\partial \vec{V}}{\partial t} + (\nabla \cdot \vec{V})\vec{V}\right] = \nabla \cdot \tilde{T} + \rho\vec{B} \tag{2}$$

$$\tilde{T} = -p\tilde{I} + \tilde{S} \tag{3}$$

where $\vec{V}, \tilde{T}, \rho, t, \vec{B}, p, \tilde{S}, \tilde{I}$ are velocity vector, Cauchy stress tensor, density, time, body force per unit volume, pressure, extra stress tensor, and unit stress tensor, respectively. Depending on the behavior of the non-Newtonian fluids, the extra stress tensor introduces various forms of nonlinearity into the equation. The extra stress tensor for the Sisko [12] fluid is given as follows:

$$\tilde{S} = \left[\hat{a} + \hat{b}\left(\sqrt{0.5\mathrm{tr}(A_1^2)}\right)^{n-1}\right]A_1 \tag{4}$$

where A_1 is the rate of deformation tensor, $\hat{a}$, $\hat{b}$, n are constants which vary for different fluids. We seek a solution of the form $(u(y), 0, 0)$ and assume the extra stress tensor to be function of $\hat{y}$ only. Using Eqs. (3) and (4) in the momentum equation of Eq. (2), the $\hat{x}$ momentum equation is obtained as follows:

$$\hat{x}\text{ - momentum} \quad -\frac{\partial \hat{p}_i}{\partial \hat{x}} + \hat{a}_i\frac{\mathrm{d}^2\hat{u}_i}{\mathrm{d}\hat{y}^2} + \hat{b}_i\frac{\mathrm{d}}{\mathrm{d}\hat{y}}\left[\frac{\mathrm{d}\hat{u}_i}{\mathrm{d}\hat{y}}\right]^n + \rho_i g\sin\theta = 0 \tag{5}$$

$$\hat{y}\text{ - momentum} \quad -\frac{\partial \hat{p}_i}{\partial \hat{y}} - \rho_i g\cos\theta = 0 \tag{6}$$

where $\hat{x}, \hat{y}$ are dimensional coordinates in the direction of the flow and in the perpendicular direction, respectively. $\hat{p}, \hat{u}$ are the pressure and the velocity components in the flow direction, g is the acceleration due to gravity, and θ is the angle of inclination of the plane. It is important to mention here that θ is maintained within the limiting value so that the laminar flow regime is ensured. With an increase in θ, the velocity increases and for a certain angle, depending on the other parameters, the flow may become turbulent. The exact range of θ varies for different situations. If the densities of the fluids are less, then the value of θ can be in the higher side and still the flow may be laminar. The specific range of θ, to maintain the flow in laminar regime, needs to be obtained from experimental investigation or from stability analysis, $i = 1, 2$ for the bottom and the top layer. For $\hat{b}_i = 0$ in Eq. (5), $\hat{a}_i$ represent the viscosities of the fluids, which is the Newtonian fluid case. n is the non-Newtonian index, which represents the measure of deviation from the Newtonian fluid. Since the flow is gravity-driven, pressure gradient in the flow direction is zero. Therefore, Eq. (5) reduces to the following form:

$$\hat{a}_i\frac{\mathrm{d}^2\hat{u}_i}{\mathrm{d}\hat{y}^2} + n\hat{b}_i\left[\frac{\mathrm{d}\hat{u}_i}{\mathrm{d}\hat{y}}\right]^{n-1}\frac{\mathrm{d}^2\hat{u}_i}{\mathrm{d}\hat{y}^2} + \rho_i g\sin\theta = 0 \tag{7}$$

Shear stress equation for Sisko fluid [12] is given as follows:

$$\hat{\tau}_i = \hat{a}_i\frac{\mathrm{d}u_i}{\mathrm{d}y} + \hat{b}_i\left(\frac{\mathrm{d}u_i}{\mathrm{d}y}\right)^n \tag{7.1}$$

From Eq. (7.1), the effective viscosity can be written as follows:

$$\mu_{\text{effective}} = \left\{\hat{a}_i + n\hat{b}_i\left[\frac{\mathrm{d}\hat{u}_i}{\mathrm{d}\hat{y}}\right]^{n-1}\right\} \tag{8}$$

To convert the governing differential equations into dimensionless form, following non-dimensional variables are introduced:

$$u_i = \frac{\hat{u}_i}{u_0}, \quad y_i = \frac{\hat{y}_i}{h}, \quad h = h_1 + h_2 \tag{9}$$

where u_0 is the reference velocity, u_i is the non-dimensional velocity in the ith layer ($i = 1$ for bottom layer and $i = 2$ for top

layer), in x-direction, and h is the length scale, respectively. Substituting these dimensionless variables in Eq. (7), the non-dimensional momentum conservation equations for the top and bottom layers are obtained as follows:

$$\frac{\mathrm{d}^2u_i}{\mathrm{d}y^2}+\frac{n\hat{b}_i}{\hat{a}_i\left(\frac{h}{u_0}\right)^{n-1}}\left(\frac{\mathrm{d}u_i}{\mathrm{d}y}\right)^{n-1}\frac{\mathrm{d}^2u_i}{\mathrm{d}y^2}+\frac{\rho_i g h^2\sin\theta}{\hat{a}_i u_0}=0 \quad (10)$$

In the present study, no predefined reference velocity exists and it needs to be identified. The third term in Eq. (10) represents the ratio of gravity force and viscous force, and for the present study, these are of the same strength. Therefore, the reference velocity can be obtained as follows:

$$u_0=\frac{\rho_1 g\sin\theta h^2}{\hat{a}} \quad (11)$$

Therefore, from Eqs. (10) and (11), the governing equation for bottom layer is obtained as follows:

$$\frac{\mathrm{d}^2u_1}{\mathrm{d}y^2}+nb_1\left(\frac{\mathrm{d}u_1}{\mathrm{d}y}\right)^{n-1}\frac{\mathrm{d}^2u_1}{\mathrm{d}y^2}+1=0 \quad (12)$$

Substituting the dimensionless variables and u_0 in Eq. (10), for the top layer, we obtain

$$\frac{\mathrm{d}^2u_2}{\mathrm{d}y^2}+nb_2\left(\frac{\mathrm{d}u_2}{\mathrm{d}y}\right)^{n-1}\frac{\mathrm{d}^2u_2}{\mathrm{d}y^2}+\frac{k_1}{k_2}=0 \quad (13)$$

where

$$b_1=\frac{\hat{b}_1}{\hat{a}_1\left(\frac{h}{u_0}\right)},\quad b_2=\frac{\hat{b}_2}{\hat{a}_2\left(\frac{h}{u_0}\right)},\quad k_1=\frac{\rho_2}{\rho_1},\quad k_2=\frac{\hat{a}_2}{\hat{a}_1} \quad (14)$$

where b_1, b_2 are the Sisko fluid parameters of the bottom and top layer fluids, respectively, and from Eq. (14), we get

$$b_2=b_1\frac{k_3}{k_2} \quad (15)$$

Two second-order ordinary differential equations (ODE) describe the flow, and to obtain the solution, four boundary conditions are required. Following boundary conditions are applicable for the two-layer flow:

$$\hat{u}_1(0)=0 \quad \text{(No slip at the plane)} \quad (16.1)$$

$$\hat{u}_1(h_1)=\hat{u}_2(h_1) \quad \text{(Continuity of velocity at the interface)} \quad (16.2)$$

$$\hat{\tau}_1(h_1)=\hat{\tau}_2(h_1) \quad \text{(Continuity of tangential stress at the interface)} \quad (16.3)$$

$$\frac{\mathrm{d}\hat{u}_2(h)}{\mathrm{d}\hat{y}}=0 \quad \text{(Zero shear at the free surface)} \quad (16.4)$$

Non-dimensional boundary conditions are as follows:

$$u_1(0)=0 \quad (17.1)$$

$$u_1(r)=u_2(r),\quad \text{where}\quad r=\frac{h_1}{h_1+h_2} \quad (17.2)$$

Using Eqs. (7.1) and (16.3), in the dimensionless form, reduces to the following:

$$\frac{\mathrm{d}u_1}{\mathrm{d}y}+b_1\left(\frac{\mathrm{d}u_1}{\mathrm{d}y}\right)^n=k_2\frac{\mathrm{d}u_2}{\mathrm{d}y}+k_3b_1\left(\frac{\mathrm{d}u_2}{\mathrm{d}y}\right)^n \quad (18.1)$$

where

$$k_3=\frac{\hat{b}_2}{\hat{b}_1}. \quad (18.2)$$

Equation (16.4), in the dimensionless form, gives

$$\frac{\mathrm{d}u_2(1)}{\mathrm{d}y}=0 \quad (18.3)$$

2.2 Solution by HPM

Equations (12) and (13) are nonlinear in nature, and HPM is an effective analytical tool for solving nonlinear ODEs. HPM is a coupling method of the homotopy theory and perturbation method introduced by He [22, 23]. It does not require the presence of any small parameter in the problem, but it can take the full advantages of the traditional perturbation method. For solving Eqs. (12) and (13), the following homotopy is constructed:

$$(1-m)\left[\frac{\mathrm{d}^2v_1}{\mathrm{d}y^2}-\frac{\mathrm{d}^2u_{10}}{\mathrm{d}y^2}\right]+m\left[\frac{\mathrm{d}^2v_1}{\mathrm{d}y^2}+nb_1\frac{\mathrm{d}^2v_1}{\mathrm{d}y^2}\left(\frac{\mathrm{d}v_1}{\mathrm{d}y}\right)^{n-1}+1\right]=0 \quad (19)$$

$$(1-m)\left[\frac{\mathrm{d}^2v_2}{\mathrm{d}y^2}-\frac{\mathrm{d}^2u_{20}}{\mathrm{d}y^2}\right]+m\left[\frac{\mathrm{d}^2v_2}{\mathrm{d}y^2}+nb_2\frac{\mathrm{d}^2v_2}{\mathrm{d}y^2}\left(\frac{\mathrm{d}v_2}{\mathrm{d}y}\right)^{n-1}+\frac{k_1}{k_2}\right]=0 \quad (20)$$

where v_1, v_2 are the approximate solutions for u_1, u_2. u_{10}, u_{20} are guess solutions for u_1, u_2, and m is an embedding parameter. In velocities u_{10}, u_{20}, the first suffix indicates the layer and the second one signifies the order (zeroth order, first order, and second order) of the solution. For example, u_{10} indicates the zeroth-order solution for the bottom layer. If $m=0$ is substituted in Eqs. (19) and (20), a simplified linear equation is produced which can be solved easily; $m=1$ reduces Eqs. (19) and (20) into the actual nonlinear equations.

v_1 and v_2 are expanded in terms of the embedding parameter m as follows:

$$v_1=v_{10}+mv_{11}+m^2v_{12}+\cdots \quad (21)$$

$$v_2 = v_{20} + m v_{21} + m^2 v_{22} + \cdots \tag{22}$$

where v_{10}, v_{11}, v_{12}, v_{20}, v_{21}, v_{22} are the approximate zeroth-order, first-order, and second-order velocities in the bottom and top layers.

To obtain the boundary conditions, we construct a homotopy for Eq. (18.1) as follows:

$$\frac{\mathrm{d}v_1}{\mathrm{d}y} - k_2\frac{\mathrm{d}v_2}{\mathrm{d}y} + m\left[b_1\left(\frac{\mathrm{d}v_1}{\mathrm{d}y}\right)^n - k_3 b_1\left(\frac{\mathrm{d}v_2}{\mathrm{d}y}\right)^n\right] = 0 \tag{23}$$

Substituting Eqs. (21) and (22) in Eqs. (19), (20), and (23) and equating the coefficients of m^0, m^1, m^2 to zero, the equations and boundary conditions for zeroth-order, first-order, and second-order system are obtained as follows.

2.2.1 Zeroth-Order Equations

$$\frac{\mathrm{d}^2 v_{10}}{\mathrm{d}y^2} - \frac{\mathrm{d}^2 u_{10}}{\mathrm{d}y^2} = 0 \tag{24}$$

$$\frac{\mathrm{d}^2 v_{20}}{\mathrm{d}y^2} - \frac{\mathrm{d}^2 u_{20}}{\mathrm{d}y^2} = 0 \tag{25}$$

Boundary Conditions

Equations (24) and (25) are second order and require two boundary conditions each for obtaining the solution. At $y = 0$ (at the plane surface), velocity is zero (the plane is at rest) because of no-slip boundary condition. From Eq. (21), we obtain zeroth-order, first-order, and second-order velocity to be zero. Therefore, the first boundary condition is obtained as follows:

$$\text{At,} \quad y = 0, \quad v_{10} = 0 \tag{26.1}$$

At the interface of the two layers, velocity is same in both layers, because velocity at a point must be same irrespective of the layers considered. Therefore, the second boundary condition is obtained by using Eqs. (21) and (22) and equating the like coefficients of like power of *m,* which is given as follows:

$$\text{At,} \quad y = r, \quad v_{10} = v_{20} \tag{26.2}$$

At the interface, in addition to the velocity, shear stress is also same irrespective of the layers considered. Using Eq. (23) and equating the coefficients of like powers of *m*, we get the zeroth-order equation for shear stress is obtained as follows:

$$\text{At,} \quad y = r, \quad \frac{\mathrm{d}v_{10}}{\mathrm{d}y} = k_2\frac{\mathrm{d}v_{20}}{\mathrm{d}y} \tag{26.3}$$

The fourth boundary condition required for solving the system equations given by Eqs. (24) and (25) is obtained from the condition of negligible shear stress at the free surface. From Eq. (23), using the condition of negligible shear stress, we obtain the boundary condition at the free surface as follows:

$$\text{At,} \quad y = 1, \quad \frac{\mathrm{d}v_{20}}{\mathrm{d}y} = 0 \tag{26.4}$$

2.2.2 First-Order Equations

$$\frac{\mathrm{d}^2 v_{11}}{\mathrm{d}y^2} + \frac{\mathrm{d}^2 u_{10}}{\mathrm{d}y^2} + n b_1 \frac{\mathrm{d}^2 v_{10}}{\mathrm{d}y^2}\left(\frac{\mathrm{d}v_{10}}{\mathrm{d}y}\right)^{n-1} + 1 = 0 \tag{27}$$

$$\frac{\mathrm{d}^2 v_{21}}{\mathrm{d}y^2} + \frac{\mathrm{d}^2 u_{20}}{\mathrm{d}y^2} + n b_2 \frac{\mathrm{d}^2 v_{20}}{\mathrm{d}y^2}\left(\frac{\mathrm{d}v_{20}}{\mathrm{d}y}\right)^{n-1} + \frac{k_1}{k_2} = 0 \tag{28}$$

Boundary Conditions

For solving Eqs. (27) and (28), four boundary conditions are required, which are obtained by following the same procedure as followed in Eqs. (26.1)–(26.4). From Eq. (21), equating the coefficient of m to zero, the first boundary condition is obtained. As the velocity in the plane surface is zero, the first-order velocity should vanish, which is given as follows:

$$\text{At,} \quad y = 0, \quad v_{11} = 0 \tag{29.1}$$

At the interface, velocity is same in both the layers, which yields the second boundary condition for the first-order problem, given as follows:

$$\text{At,} \quad y = r, \quad v_{11} = v_{21} \tag{29.2}$$

Equality of shear stress at the interface produces the third boundary condition for the first-order problems as follows:

$$\text{At,} \quad y = r, \quad \frac{\mathrm{d}v_{11}}{\mathrm{d}y} + b_1\left(\frac{\mathrm{d}v_{10}}{\mathrm{d}y}\right)^n = k_2\frac{\mathrm{d}v_{21}}{\mathrm{d}y} + k_3 b_1\left(\frac{\mathrm{d}v_{20}}{\mathrm{d}y}\right)^n \tag{29.3}$$

The negligible (zero) shear at the free surface yields the fourth boundary condition for the first-order problem, given as follows:

$$\text{At,} \quad y = 1, \quad \frac{\mathrm{d}v_{21}}{\mathrm{d}y} = 0 \tag{29.4}$$

2.2.3 Second-Order Equations

$$\begin{aligned}&\frac{\mathrm{d}^2 v_{12}}{\mathrm{d}y^2} + n(n-1) b_1 \frac{\mathrm{d}^2 v_{10}}{\mathrm{d}y^2}\left(\frac{\mathrm{d}v_{10}}{\mathrm{d}y}\right)^{n-2}\frac{\mathrm{d}v_{11}}{\mathrm{d}y} \\ &\quad + n b_1 \frac{\mathrm{d}^2 v_{11}}{\mathrm{d}y^2}\left(\frac{\mathrm{d}v_{10}}{\mathrm{d}y}\right)^{n-1} = 0 \\ &\frac{\mathrm{d}^2 v_{22}}{\mathrm{d}y^2} + n(n-1) b_2 \frac{\mathrm{d}^2 v_{20}}{\mathrm{d}y^2}\left(\frac{\mathrm{d}v_{20}}{\mathrm{d}y}\right)^{n-2}\frac{\mathrm{d}v_{21}}{\mathrm{d}y}\end{aligned} \tag{30}$$

$$+nb_2\frac{d^2v_{21}}{dy^2}\left(\frac{dv_{20}}{dy}\right)^{n-1}=0 \tag{31}$$

Boundary Conditions

Four boundary conditions are required for solving the second-order problem, which are obtained using the condition of no slip at the plane surface, equality of velocity at the interface, equality of shear stress at the interface, and the vanishing of shear stress at the free surface, as discussed in Eqs. (26.1)–(26.4) and in Eqs. (29.1)–(29.4). From no-slip condition, we get the first equation as follows:

$$\text{At,}\quad y=0,\quad v_{12}=0 \tag{32.1}$$

From equality of velocity at the interface, second equation is obtained, which is as follows:

$$\text{At,}\quad y=r,\quad v_{12}=v_{22} \tag{32.2}$$

From the condition of equality of shear stress, the third condition is obtained, given as follows:

$$\text{At,}\quad y=r,\quad \frac{dv_{12}}{dy}+nb_1\left(\frac{dv_{10}}{dy}\right)^{n-1}\frac{dv_{11}}{dy}=k_2\frac{dv_{22}}{dy}+nk_3b_1\left(\frac{dv_{20}}{dy}\right)^{n-1}\frac{dv_{21}}{dy} \tag{32.3}$$

Vanishing of the shear at the free surface generates the last boundary condition, given as follows:

$$\text{At,}\quad y=1,\quad \frac{dv_{22}}{dy}=0 \tag{32.4}$$

2.2.4 Zeroth-Order Solutions

Guess solutions are selected, satisfying the boundary conditions given by Eqs. (26.1)–(26.4) as follows:

$$u_{10}=-\frac{y^2}{2(1+b_1)}+c_1y \tag{33}$$

$$u_{20}=-\frac{y^2k_1}{2(1+b_2)k_2}+c_3y+c_4 \tag{34}$$

where

$$c_3=\frac{k_1}{(1+b_2)k_2} \tag{35.1}$$

$$c_1=\frac{r}{(1+b_1)}+\frac{k_1(1-r)}{(1+b_2)} \tag{35.2}$$

$$c_4=c_1r-\frac{r^2}{(1+b_1)2}+\frac{k_1}{(1+b_2)k_2}\left(\frac{r^2}{2}-r\right) \tag{35.3}$$

From Eqs. (24) and (25), the solutions of the zeroth-order equations are obtained as follows:

$$v_{10}=-\frac{y^2}{2(1+b_1)}+c_1y \tag{36}$$

$$v_{20}=-\frac{y^2k_1}{2(1+b_2)k_2}+c_3y+c_4 \tag{37}$$

2.2.5 First-Order Solution

Equations (36) and (37) are substituted in Eqs. (27) and (28), and first-order solutions are obtained satisfying the boundary conditions given by Eqs. (29.1)–(29.4). The solutions are:

$$v_{11}=-\frac{y^2b_1}{2(1+b_1)}+\frac{b_1(1+b_1)}{(n+1)}\left(c_1-\frac{y}{(1+b_1)}\right)^{n+1}+c_5y+c_6 \tag{38}$$

$$v_{21}=-\frac{y^2b_2k_1}{2(1+b_2)k_2}+\frac{b_2(1+b_2)k_2}{(n+1)k_1}\left(c_3-\frac{k_1y}{k_2(1+b_2)}\right)^{n+1}+c_7y+c_8 \tag{39}$$

$$c_5=\frac{k_1b_2(1-r)}{(1+b_2)}+\frac{b_1r}{(1+b_1)} \tag{40.1}$$

$$c_6=-\frac{b_1(1+b_1)}{(n+1)}\left[\frac{r}{(1+b_1)}+\frac{k_1(1-r)}{(1+b_2)}\right]^{n+1} \tag{40.2}$$

$$c_7=\frac{k_1b_2}{k_2(1+b_2)} \tag{40.3}$$

$$c_8=-\frac{b_1r^2}{(1+b_1)2}+\frac{b_1(1+b_1)}{(1+n)2}\left(c_1-\frac{r}{(1+b_1)}\right)^{n+1}+c_5r+c_6+\frac{k_1b_2r^2}{k_2(1+b_2)2}\frac{k_2b_2(1+b_2)}{k_1(1+n)}\left(c_3-\frac{k_1r}{k_2(1+b_2)}\right)^{n+1}-c_7r \tag{40.4}$$

2.2.6 Second-Order Solution

Equations (38) and (39) are substituted in Eqs. (30) and (31), and satisfying the boundary conditions given by Eqs. (32.1)–(32.4), the second-order solutions are obtained as follows:

$$v_{12}=\left(b_1c_5-b_1^2c_1\right)(1+b_1)\left(c_1-\frac{y}{(1+b_1)}\right)^n+\left(\frac{n-1}{n+1}\right)b_1^2(1+b_1)\left(c_1-\frac{y}{(1+b_1)}\right)^{n+1}-\frac{(n-1)b_1^2}{2(2n-1)}\left(c_1-\frac{y}{(1+b_1)}\right)^{2n}(1+b_1)+c_9y+c_{10} \tag{41}$$

$$v_{22} = \left(b_2c_7 - b_2^2c_3\right)\left(\frac{k_2}{k_1}\right)(1+b_2)\left(c_3 - \frac{k_1 y}{k_2(1+b_2)}\right)^n + \left(\frac{n-1}{n+1}\right)b_2^2(1+b_2)\left(\frac{k_2}{k_1}\right)\left(c_3 - \frac{k_1 y}{k_2(1+b_2)}\right)^{n+1} - \frac{(n-1)b_2^2}{2(2n-1)}\left(\frac{k_2}{k_1}\right)(1+b_2)\left(c_3 - \frac{k_1 y}{k_2(1+b_2)}\right)^{2n} + c_{11}y + c_{12} \tag{42}$$

Therefore, the expressions for the velocity in bottom and top layers are found to be:

$$u_1 = v_1 = v_{10} + v_{11} + v_{12} \quad \text{(substituting } m = 1 \text{ in Eq. (21))} \tag{44}$$

$$u_2 = v_2 = v_{20} + v_{21} + v_{22} \quad \text{(substituting } m = 1 \text{ in Eq. (22))} \tag{45}$$

$$c_9 = n\left(b_1c_5 - b_1^2c_1\right)\left(c_1 - \frac{r}{(1+b_1)}\right)^{n-1} + (n-1)b_1^2\left(c_1 - \frac{r}{(1+b_1)}\right)^n - \frac{(n-1)nb_1^2}{(2n-1)}\left(c_1 - \frac{r}{(1+b_1)}\right)^{2n-1} + k_2\left[\frac{n(n-1)b_2^2}{(2n-1)}\left\{c_3 - \frac{k_1 r}{k_2(1+b_2)}\right\}^{2n-1} - n\left(b_2c_7 - b_2^2c_3\right)\left(c_3 - \frac{k_1 r}{k_2(1+b_2)}\right)^n - (n-1)b_2^2\left(c_3 - \frac{k_1 r}{k_2(1+b_2)}\right)^n + c_{11}\right] \tag{43.1}$$

$$c_{10} = \frac{(n-1)b_1^2c_1^{2n}(1+b_1)}{2(2n-1)} - \frac{(n-1)b_1^2}{(n+1)}(1+b_1)c_1^{n+1} + (1+b_1)\left(b_1c_5 - b_1^2c_1\right)c_1^n \tag{43.2}$$

$$c_{11} = -\frac{n(n-1)b_2^2}{(2n-1)}\left\{c_3 - \frac{k_1 r}{k_2(1+b_2)}\right\}^{2n-1} + n\left(b_2c_7 - b_2^2c_3\right)\left\{c_3 - \frac{k_1}{k_2(1+b_2)}\right\}^{n-1} + (n-1)b_2^2\left\{c_3 - \frac{k_1}{k_2(1+b_2)}\right\}^n \tag{43.3}$$

$$c_{12} = \left(b_1c_5 - b_1^2c_1\right)(1+b_1)\left(c_1 - \frac{r}{(1+b_1)}\right)^n + \frac{(n-1)b_1^2(1+b_1)}{(n+1)}\left(c_1 - \frac{r}{(1+b_1)}\right)^n - \frac{(n-1)nb_1^2}{(2n-1)}\left(c_1 - \frac{r}{(1+b_1)}\right)^{n+1} - \frac{(n-1)b_1^2(1+b_1)}{2(2n-1)}\left\{c_1 - \frac{r}{(1+b_1)}\right\}^{2n} + c_9r + c_{10} - \left(b_2c_7 - b_2^2c_3\right)(1+b_2)\left(\frac{k_2}{k_1}\right)\left(c_3 - \frac{k_1 r}{k_2(1+b_2)}\right)^n - \frac{(n-1)b_2^2(1+b_2)}{(n+1)}\left(\frac{k_2}{k_1}\right)\left(c_3 - \frac{k_1 r}{k_2(1+b_2)}\right)^{n+1} + \frac{(n-1)b_2^2(1+b_2)}{2(2n-1)}\left(\frac{k_2}{k_1}\right)\left\{c_3 - \frac{k_1 r}{k_2(1+b_2)}\right\}^{2n} - c_{11}r \tag{43.4}$$

2.3 Exact Solution for $n = 2$

The governing equations are nonlinear, and they do not have any closed-form solution for all values of n. However, for the special cases of $n = 1$ and 2, exact solutions are available. But, $n = 1$ represents the case for the Newtonian fluids and can easily be obtained. Here, the exact solution for $n = 2$ is presented. Through a suitable substitution in Eq. (12), the solution can be obtained as follows:

$$u_1 = \frac{0.5}{b_1}\left[-y - \frac{1}{6b_1}\{1 - 4b_1(y - c_1)\}^{3/2}\right] + c_2 \tag{46}$$

Similar procedure is followed to solve u_2 from Eq. (13) to obtain:

$$u_2 = \frac{0.5}{b_2}\left[-y - \frac{1}{6b_2\left(\frac{k_1}{k_2}\right)}\left\{1 - 4b_2\left(\frac{k_1}{k_2}y - c_1\right)\right\}^{3/2}\right] + c_4 \tag{47}$$

where c_1, c_2, c_3, c_4 are evaluated from the boundary conditions given by Eqs. (18.1)–(18.3). The details of the solution procedure of the governing equation and the evaluation of the boundary conditions are given in "Appendix A."

3 Results and Discussion

In this section, at first, a comparison between the results from the analytical solution and those obtained from the exact solution is made. Then, the results from the analytical solution are presented graphically. The property ratios of the two fluids have been varied widely to investigate the effect of such variation on the velocity.

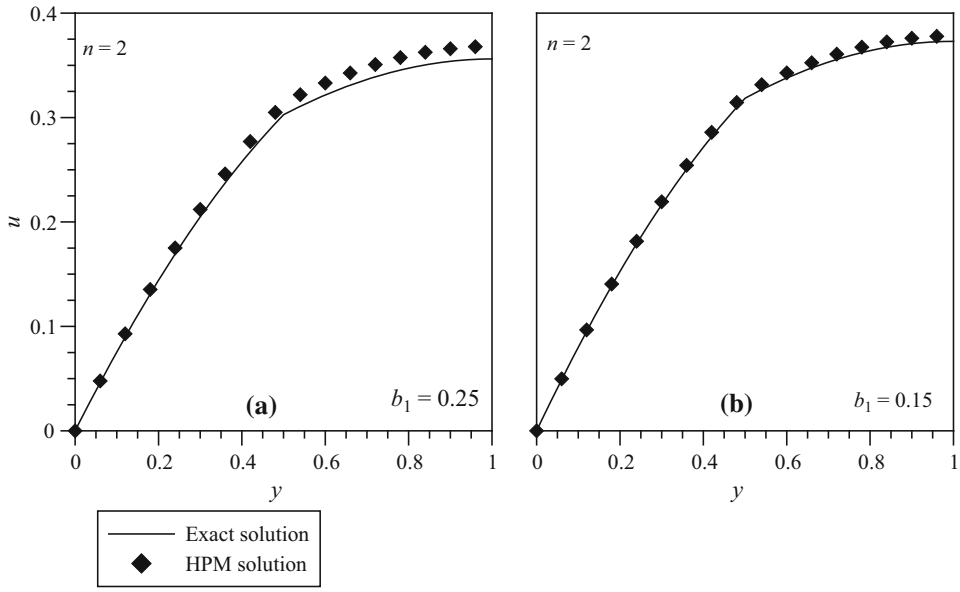

Fig. 2 Comparison between the dimensionless velocity distribution from the analytical results and from the exact solution for $n = 2$, $k_1 = 0.9$, $k_2 = 2$, $k_3 = 3$, and $b_1 = 0.25$ and 0.15

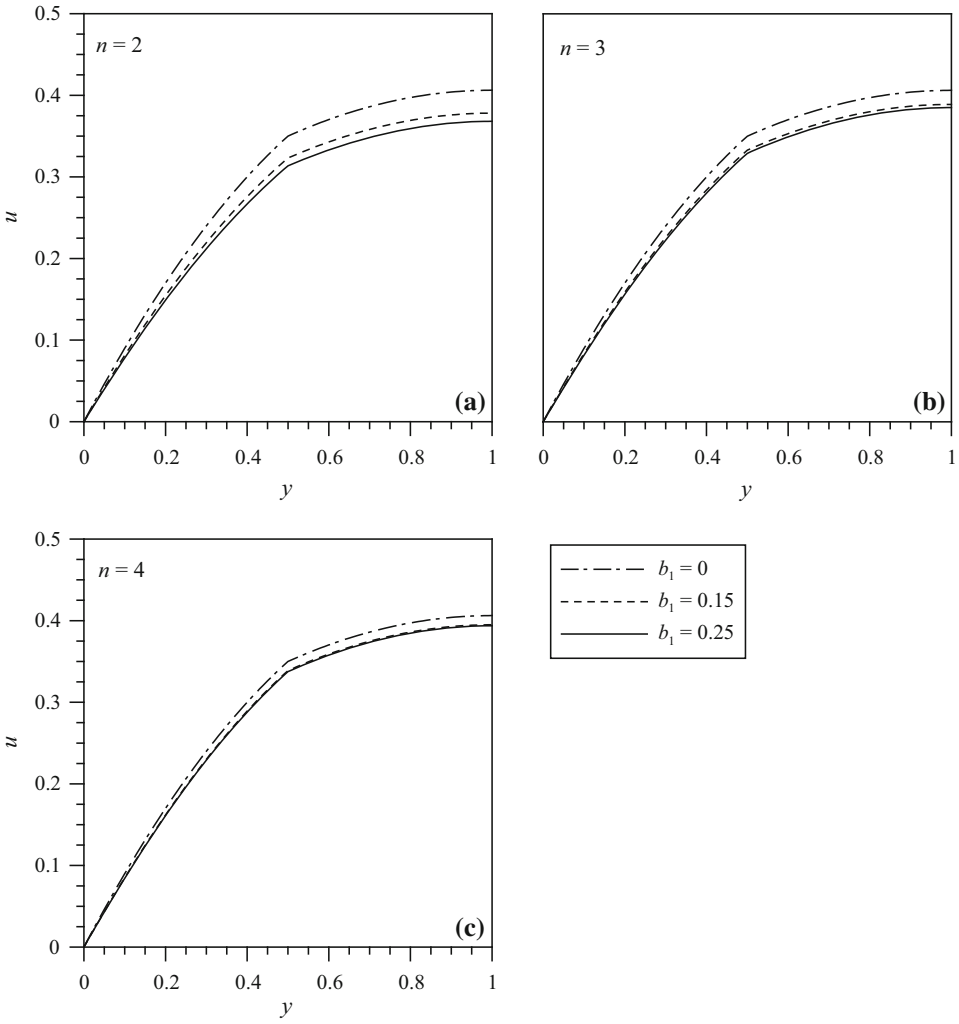

Fig. 3 Dimensionless velocity distribution for $b_1 = 0$, 0.15, 0.25 and for **a** $n = 2$, **b** $n = 3$, and **c** $n = 4$ and $k_1 = 0.9$, $k_2 = 2$, $k_3 = 3$

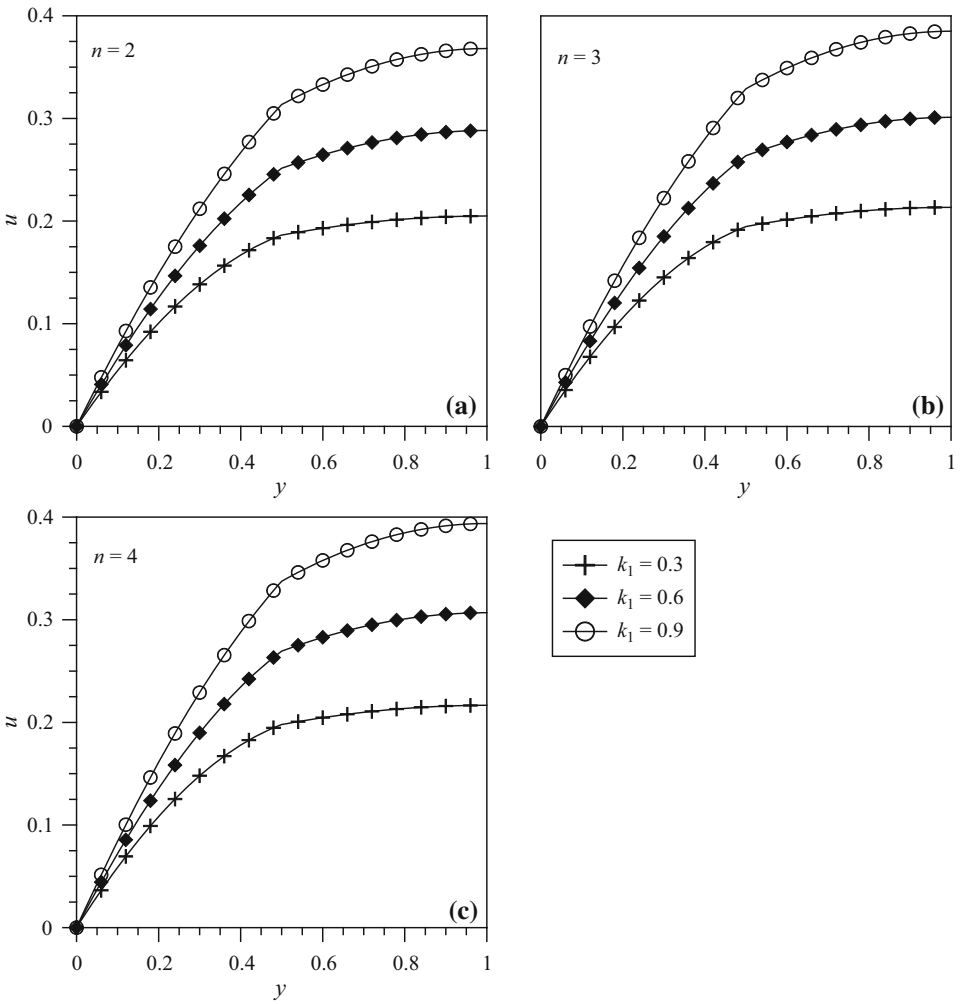

Fig. 4 Velocity distribution for $k_1 = 0.3, 0.6, 0.9$ and for **a** $n = 2$, **b** $n = 3$, and **c** $n = 4$ and $b_1 = 0.25$ and $k_2 = 2$, $k_3 = 3$

In Fig. 2, the non-dimensional velocity distributions from the exact solution Eqs. (46) and (47) for the Sisko fluid with the non-Newtonian index $n = 2$ and from the analytical solution Eqs. (44) and (45) are compared graphically for two different values of b_1 while keeping other parameters same. It is evident from the figure that the results of the analytical solution are in close agreement with those obtained from the exact solution. Figure 2a displays the comparison between the results of HPM and exact solution when $b_1 = 0.25$. The percentage of maximum error (in the free surface) is 5.6%. The percentage error decreases with a decrease in b_1 as shown in Fig. 2b. The discrepancy in the results is zero in the plane surface (velocity is zero because of no-slip condition) and gradually increases as the distance from the plane surface increases. The discrepancy is maximum at the free surface.

Figure 3 depicts the non-dimensional velocity distribution from the analytical solution for different values of the non-Newtonian index n and the Sisko fluid parameter b_1. It is evident that the velocity in both the layers of the fluid decreases with an increase in the values of b_1. It may be noted that an increase in b_1 can be interpreted in two ways. For fixed values of $\hat{a}_1$, higher values of $\hat{b}_1$ result in an increase in b_1. As $\hat{b}_1$ increases, from Eq. (8), it is clear that the effective viscosity increases which results in a decrease in the velocity for the gravity-driven flow. It is evident from the figure that the change in velocity is comparatively higher near the top layer. The presence of the solid surface suppresses any significant change in the vicinity of the plane surface. In this context, to demonstrate how the results of the present study can be used in real-life situation, a two-layer gravity-driven flow of Sisko fluids has been considered. In the absence of the data from experiments on Sisko fluids, realistic values of the properties and parameters involved are considered. The following values are used:

$h_1 = 10$ mm, $h_2 = 10$ mm, $\theta = 20°$, $a_1 = 100$ kg/m s, $a_2 = 300$ kg/m s, $b_1 = 100$ kg s^{n-2}/m, $b_2 = 300$ kg s^{n-2}/m, $\rho_1 = 900$ kg/m^3, $\rho_2 = 700$ kg/m^3, $n = 2$.

From Eqs. (11) and (14), we obtain $u_0 = 0.003$ m/s, $b_1 = 0.30$, $b_2 = 0.225$. If the threshold velocity, obtained from experiment or from stability analysis, is = 5 mm/s, then from Fig. 3a, the maximum non-dimensional velocity is obtained as 0.4, which yields dimensional velocity to be 1.2 mm/s. If

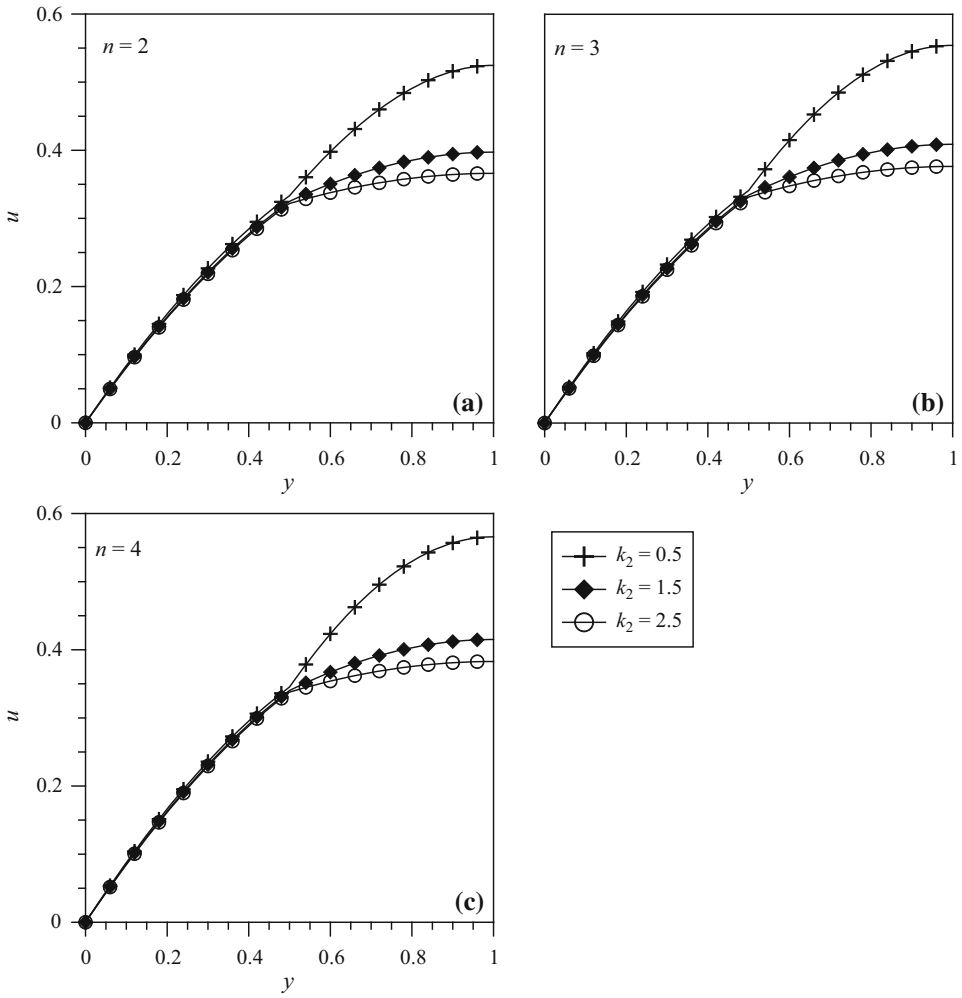

Fig. 5 Velocity distribution for $k_2 = 0.5$, 1.5, 2.5 and **a** $n = 2$, **b** $n = 3$, and **c** $n = 4$ for $k_1 = 0.9$, $b_1 = 0.15$, and $k_3 = 3$

the velocity crosses the threshold value or approaches near this, by changing the values of a_1, a_2, b_1, b_2, ρ_1, h_1, and h_2, the maximum velocity can be controlled and maintained well below the limiting value. In this way, by changing the properties of the fluids, different fluids can be selected for controlling the velocity.

Figure 4 presents the dimensionless velocity distributions for different values of the non-Newtonian index n and the density ratio k_1 as a parameter. It is evident from the figure that an increase in the density ratio of the top and bottom layer fluid causes significant increase in the velocity in the top layer. In the bottom layer, increase in the velocity is less near the plane due to the presence of the solid surface as discussed earlier. As the density ratio increases, the higher body force results in a significant increase in the velocity. It is important to note that the non-dimensional velocity increases slightly with an increase in n, as indicated in Fig. 4a–c. From Eq. (8), it is evident that an increase in n results in an increase in the effective viscosity of the fluid which should cause a decrease in the velocity. The reverse trend displayed by the figures can be explained as follows. The Sisko fluid parameters b_1 and b_2, as defined in Eq. (14), have u_0 in the numerator. Any increase in n causes an increase in the numerator. If the values of b_1 and b_2 are maintained, fixed values of $\hat{b}_1$, $\hat{b}_2$ have to decrease. The effect of $\hat{b}_1$, $\hat{b}_2$ on velocity is more dominant than the influence of n. Therefore, the non-dimensional velocities are observed to increase with an increase in n.

Dimensionless velocity distribution for different values of n and k_2 is depicted in Fig. 5. The results imply that with an increase in k_2, the velocity decreases. As discussed earlier, once u_0 is chosen, $\frac{du_1}{dy} = z_1$ becomes fixed. Therefore, an increase in k_2 can be caused only due to an increase in $\frac{dz_1}{dy} + 2b_1 z_1 \frac{dz_1}{dy} + 1 = 0$. Increase in k_2 signifies increase in the effective viscosity ratio which results in a decrease in the velocity. Compared to the density ratio, the effect of k_2 on the velocity is relatively less.

The effect of the thickness ratio on the non-dimensional velocity distribution is presented in Fig. 6. The results indicate an increase in the velocity in the top layer and a decrease in the velocity in the bottom layer with an increase in the thickness ratio. The force due to gravity decreases in the

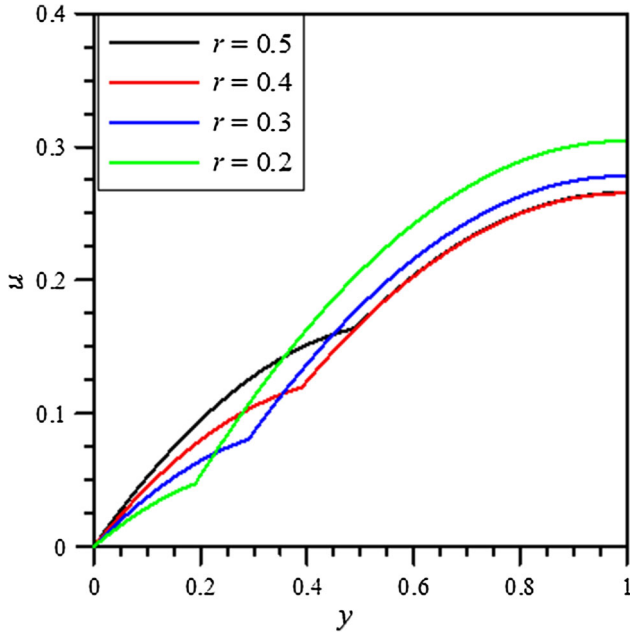

Fig. 6 Non-dimensional velocity distribution for different r when $b_1 = 0.1$, $k_1 = 0.2$, $k_2 = 0.25$, and $k_3 = 0.1$

bottom layer as the thickness of the bottom layer decreases, which leads to the lower velocity in the bottom layer.

4 Conclusions

Single-layer thin film gravity-driven flow of non-Newtonian fluid has been studied by the researchers, but thin film gravity-driven flow of multilayer non-Newtonian Sisko fluids has never been considered before, as revealed by the open literature. This kind of flow, however, is important in multilayer coating process. In the present study, thin film gravity-driven flow of two immiscible non-Newtonian Sisko fluids has been examined for the first time. A closed-form analytical solution of two-layer flow of typical Sisko fluids down a flat inclined plane is obtained for a special case, and for other cases of the non-Newtonian index, approximate analytical solution is yielded by solving the governing equations employing He's homotopy perturbation method. Considering a wide variation of the property ratios of the two fluids, the flow behavior (distribution of velocity) in the two layers has been investigated. Following important observations are made:

The velocity distribution is the most sensitive toward any change in density ratio of the top and bottom fluid layers. A 100% increase in the non-dimensional velocity is observed at all the points when the density ratio increases by around three times. At lower values of the density ratio, the velocity in the top layer is practically constant. However, in the bottom layer, a significant change in velocity is observed at different points. With an increase in the Sisko fluid parameter, the velocity decreases significantly in both the layers. For higher values of the non-Newtonian index n, however, the effect of the Sisko fluid parameter b diminishes on the velocity distribution as depicted in the figures. An increase in the value of k_2 results in a decrease in the velocity; this decrease is significant in the top layer. In the bottom layer, the nonlinearity of the velocity distribution is much less due to the effect of the solid wall. Velocity in the bottom layer decreases, and in the top layer, velocity increases with an increase in the thickness ratio.

Using the results of the present study, the maximum velocity in the layers can be controlled so that the threshold velocity, at which flow is unstable, is never reached and quality of the coating is ensured. The threshold velocity can be obtained from the experimental investigation. The parameters such as density ratio, viscosity ratio, and ratio of thickness can be varied accordingly to maintain the velocity in each layer much lower than the threshold limit. Further, Sisko fluids with different properties and non-Newtonian index can be selected to obtain the required density ratio or viscosity ratio, required for limiting the velocity lower than the limiting value. Moreover, the thickness ratio can be varied to maintain the velocity. However, the limitation of the present study is the inability to fix the number of layers required to achieve the velocity as only two layers are considered. But, the study can further be extended to more than bilayer case following the similar procedure adopted in the present investigation. The practical application of the present study is that it can be used for multilayer coating purposes.

Appendix A

Equation (12) is solved by substituting

$$\frac{\mathrm{d}u_1}{\mathrm{d}y} = z_1 \tag{A.1}$$

which gives:

$$\frac{\mathrm{d}z_1}{\mathrm{d}y} + 2b_1 z_1 \frac{\mathrm{d}z_1}{\mathrm{d}y} + 1 = 0 \tag{A.2}$$

$$\Rightarrow \frac{\mathrm{d}z_1}{\mathrm{d}y}(1 + 2b_1 z_1) = -\mathrm{d}y \tag{A.3}$$

Integrating Eq. (A.3) and solving, we get: $z_1 = \frac{-1+\sqrt{1-4b_1(y-c_1)}}{2b_1}$ (taking the +ve value for $\frac{du_1}{dy}$, as u_1 increases with y)

$$=> \frac{du_1}{dy} = \frac{-1+\sqrt{1-4b_1(y-c_1)}}{2b_1} \tag{A.4}$$

$$=> u_1 = \frac{0.5}{b_1}\left[-y - \frac{1}{6b_1}\{1-4b_1(y-c_1)\}^{3/2}\right] + c_2 \tag{A.5}$$

$$-1+\sqrt{1-4b_2\left(\frac{k_1}{k_2}-c_3\right)} = 0 \tag{A.10}$$

$c_3 = \frac{k_1}{k_2}$. These four equations are solved for c_1, c_2, c_3, and c_4, and velocity in both layers is found as follows:

$$c_3 = \frac{k_1}{k_2} \tag{A.11}$$

$$c_1 = r - \frac{1}{4b_1}\left[1 - \left\{0.5 + \sqrt{0.25 + b_1\left\{\begin{array}{l} 0.5k_2\frac{b_1}{b_2}\left(-1+\sqrt{1-4b_2\left(\frac{k_1}{k_2}\right)(r-1)}\right) \\ +0.25b_1k_3\left(-1+\sqrt{1-4b_2\left(\frac{k_1}{k_2}\right)(r-1)}\right)^2 \end{array}\right\}}\right\}\right] \tag{A.12}$$

Similar procedure is used to solve u_2 from Eq. (13) which gives the solution as follows:

$$u_2 = \frac{0.5}{b_2}\left[-y - \frac{1}{6b_2\left(\frac{k_1}{k_2}\right)}\left\{1-4b_2\left(\frac{k_1}{k_2}y - c_1\right)\right\}^{3/2}\right] + c_4 \tag{A.6}$$

Now, using the boundary conditions given by Eqs. (17.1, 17.2), we get the following equations:

$$\frac{0.5}{b_1}\left[-\frac{1}{6b_1}\{1+4b_1c_1\}^{3/2}\right] + c_2 = 0 \tag{A.7}$$

$$\frac{0.5}{b_1}\left[-r - \frac{1}{6b_1}\{1-4b_1(r-c_1)\}^{3/2}\right] + c_2 = \frac{0.5}{b_2}\left[-r - \frac{1}{6b_2\left(\frac{k_1}{k_2}\right)}\left\{1-4b_2\left(\frac{k_1}{k_2}r - c_3\right)\right\}^{3/2}\right] + c_4 \tag{A.8}$$

$$\frac{0.5}{b_1}\left[-1+\sqrt{1-4b_1(r-c_1)}\right] + \frac{(0.5)^2}{b_1}\left[-1+\sqrt{1-4b_1(r-c_1)}\right]^2 = \frac{0.5}{b_2}k_2\left[-1+\sqrt{1-4b_2\left(\frac{k_1}{k_2}r - c_3\right)}\right] + \frac{(0.5)^2}{(b_2)^2}b_1k_3\left[-1+\sqrt{1-4b_2\left(\frac{k_1}{k_2}r - c_3\right)}\right]^2 \tag{A.9}$$

$$c_2 = \frac{-0.5}{6b_1}\{1+4b_1c_1\} \tag{A.13}$$

$$c_4 = \frac{0.5}{b_1}\left[-r - \frac{1}{6b_1}\{1-4b_1(r-c_1)\}^{3/2}\right] + c_2 - \frac{0.5}{b_2}\left[-r - \frac{1}{6b_2\left(\frac{k_1}{k_2}\right)}\left\{1-4b_2\left(\frac{k_1}{k_2}r - c_3\right)\right\}^{3/2}\right] \tag{A.14}$$

References

1. Bontozoglou, V.; Papapolymerou, G.: Laminar film down a wavy incline. Int. J. Multiph. Flow **23**, 69–79 (1997)
2. Kang, F.; Chen, K.P.: Gravity-driven two layer flow down a slightly wavy periodic incline at low Reynolds number. Int. J. Multiph. Flow **21**, 501–513 (1995)
3. Pozrikidis, C.: The flow of a liquid film along a periodic wall. J. Fluid Mech. **188**, 275–300 (1988)
4. Amaouche, M.; Djema, A.; Bourdache, L.: A modified Shkadov's model for thin film flow of a power law fluid over an inclined surface. Comptes Rendus Mec. **337**, 48–52 (2009)
5. Kheyfets, V.O.; Kieweg, S.L.: Gravity-driven thin film flow of an ellis fluid. J. Non-Newton. Fluid Mech. **202**, 88–98 (2013)
6. Alam, M.K.; Rahim, M.T.; Avital, E.J.; Islam, S.; Siddiqui, A.M.; Williams, J.J.R.: Solution of the steady thin film flow of non-Newtonian fluid on vertical cylinder using Adomian Decomposition Method. J. Frankl. Inst. **350**, 818–839 (2013)
7. Singla, R.K.; Das, R.: Adomian decomposition method for a stepped fin with all temperature dependent modes of heat transfer. Int. J. Heat Mass Transf. **82**, 447–459 (2015)
8. Siddiqui, A.M.; Mahmood, R.; Ghori, Q.K.: Homotopy perturbation method for thin film flow of a third grade fluid down an inclined plane. Chaos Solitons Fractals **35**, 140–147 (2008)
9. Hayat, T.; Ellahi, R.; Mahmood, F.M.: Exact solutions for thin film flow of a third grade fluid down an inclined plane. Chaos Solitons Fractals **38**, 1336–1341 (2008)

10. Kumaran, V.; Tamizharasi, R.; Merkin, J.H.; Vajravelu, K.: On thin film flow of a third-grade fluid down an inclined plane. Arch. Appl. Mech. **82**, 261–266 (2012)
11. Sisko, A.W.: The flow of lubricating greases. Ind. Eng. Chem. Res. **50**, 178–179 (1958)
12. Khan, M.I.; Hayat, T.; Qayyum, S.; Khan, M.I.; Alsaedi, A.: Entropy generation (irreversibility) associated with flow and heat transport mechanism in Sisko nanomaterial. Phys. Lett. A **382**, 2343–2353 (2018)
13. Shah, R.A.; Gaskell, P.; Veremieiev, S.: Free surface thin film flow of a Sisko's fluid over a surface topography. J. Appl. Fluid Mech. **10**, 307–317 (2017)
14. Khan, M.; Shahzad, A.: On boundary layer flow of a Sisko fluid over a stretching sheet. Quaest. Math. **36**, 137–151 (2013)
15. Khan, M.; Malik, R.; Munir, A.: Mixed convective heat transfer to a Sisko fluid over a radially stretching sheet in presence of convective boundary conditions. AIP Adv. **5**, 087178 (2015)
16. Nadeem, S.; Akbar, N.S.; Vajravelu, K.: Peristaltic flow of a Sisko fluid in an endoscope: analytical and numerical solutions. Int. J. Comput. Math. **88**, 1013–1023 (2011)
17. Haghighi, A.R.; Asadi Chalak, S.: Mathematical modeling of Sisko fluid flow through a stenosed artery. Int. J. Ind. Math. **9**, 75–82 (2017)
18. Siddiqui, A.M.; Ahmed, M.; Ghori, Q.K.: Thin film flow of non-Newtonian fluids on a moving belt. Chaos, Solitons Fractals **33**, 1006–1016 (2007)
19. Hajmohammadai, M.R.; Nourazar, S.S.: On the insertion of a thin gas layer in micro cylindrical Couette flows involving power-law liquids. Int. J. Heat Mass Transf. **75**, 97–108 (2014)
20. Cuce, E.; Cuce, P.M.: A successful application of homotopy perturbation method for efficiency and effectiveness assessment of longitudinal porous fins. Energy Convers. Manag. **93**, 92–99 (2015)
21. Torabi, M.; Zhang, Q.B.: Analytical solution for evaluating the thermal performance and efficiency of convective-radiative straight fins with various profiles and considering all non-linearities. Energy Convers. Manag. **66**, 199–210 (2013)
22. He, J.H.: A new approach to non-linear partial differential equations. Commun. Nonlinear Sci. Numer. Simul. **2**, 230–235 (1997)
23. He, J.H.: A coupling method of homotopy perturbation technique and a perturbation technique for non-linear problem. Int. J. Non-linear Mech. **135**, 73–79 (2000)